

# Kinetic Rate Comparison of Methane Catalytic Combustion of Palladium Catalysts Impregnated onto $\gamma$ -Alumina and Bio-Char

Noor S. Nasri, Eric C. A. Tatt, Usman D. Hamza, Jibril Mohammed, Husna M. Zain

**Abstract**—Catalytic combustion of methane is imperative due to stability of methane at low temperature. Methane ( $\text{CH}_4$ ), therefore, remains unconverted in vehicle exhausts thereby causing greenhouse gas GHG emission problem. In this study, heterogeneous catalysts of palladium with bio-char (2 wt% Pd/Bc) and  $\text{Al}_2\text{O}_3$  (2wt% Pd/  $\text{Al}_2\text{O}_3$ ) supports were prepared by incipient wetness impregnation and then subsequently tested for catalytic combustion of  $\text{CH}_4$ . Support-porous heterogeneous catalytic combustion (HCC) material were selected based on factors such as surface area, porosity, thermal stability, thermal conductivity, reactivity with reactants or products, chemical stability, catalytic activity, and catalyst life. Sustainable and renewable support-material of bio-mass char derived from palm shell waste material was compared with those from the conventional support-porous materials. Kinetic rate of reaction was determined for combustion of methane on Palladium (Pd) based catalyst with  $\text{Al}_2\text{O}_3$  support and bio-char (Bc). Material characterization was done using TGA, SEM, and BET surface area. The performance test was accomplished using tubular quartz reactor with gas mixture ratio of 3% methane and 97% air. The methane porous-HCC conversion was carried out using online gas analyzer connected to the reactor that performed porous-HCC. BET surface area for prepared 2 wt% Pd/Bc is smaller than prepared 2wt% Pd/  $\text{Al}_2\text{O}_3$  due to its low porosity between particles. The order of catalyst activity based on kinetic rate on reaction of catalysts in low temperature was 2wt% Pd/Bc>calcined 2wt% Pd/  $\text{Al}_2\text{O}_3$ > 2wt% Pd/  $\text{Al}_2\text{O}_3$ >calcined 2wt% Pd/Bc. Hence agro waste material can successfully be utilized as an inexpensive catalyst support material for enhanced  $\text{CH}_4$  catalytic combustion.

**Keywords**—Catalytic-combustion, Environmental, Support-bio-char material, Sustainable, Renewable material.

## I. INTRODUCTION

GENERALLY, climate change has becoming a global environmental issue that may trigger irreversible changes in the environment with catastrophic consequences for human,

Noor S. Nasri is the Director with the Sustainability Waste-To-Wealth Unit, UTM-MPRC Institute for Oil and Gas, Energy Research Alliance, Universiti Teknologi Malaysia, 81310 UTM Johor Bahru, Johor, Malaysia (phone: +(6)07-5535570, Fax: +(6)07-5545667; e-mail: noorshaw@petroleum.utm.my).

Eric C. A. Tatt is with the Sustainability Waste-To-Wealth Unit, UTM-MPRC Institute for Oil and Gas, Energy Research Alliance, Universiti Teknologi Malaysia, 81310 UTM Johor Bahru, Johor, Malaysia (e-mail: eric.chew1231@gmail.com).

Usman D. Hamza and Jibril Mohammed are lecturers at the Chemical Engineering Department, Abubakar Tafawa Balewa University, Tafawa Balewa Way, PMB 0248 Bauchi, Bauchi state, Nigeria (e-mails: usmandhamza@yahoo.com, jibrilmuhammad@gmail.com).

Husna M. Zain is a master's student at Faculty of Petroleum and Renewable Energy Engineering, Universiti Teknologi Malaysia, 81310 UTM Johor Bahru, Johor, Malaysia (e-mail: husnae@yahoo.com).

animals and plants on our planet. The main factor for global warming is likely due to increase of greenhouse gas (GHG) emission such as methane ( $\text{CH}_4$ ), carbon dioxide ( $\text{CO}_2$ ) and nitrous oxide ( $\text{NO}_x$ ) [1]. In fact, thermal combustion of natural gas (composed mainly of methane), a method which is commonly used to produce thermal energy for electricity generation has causes emissions of significant amounts of GHG [2]. Hence, reduction of GHG emission has become main concern of many countries to create greener environment. For example, ratification of Kyoto Protocol by 192 parties to combat climate change with an aim to deliver a 5 percent reduction in emissions compared with 1990. Therefore, catalytic combustion of methane (CCM) has very attractive characteristics compared with thermal combustion. The combustion temperature is lower and combustion is performed at a concentration range outside of flammability limits, due to the complete oxidation property. As a result, almost no  $\text{NO}_x$ , CO or particulate matter can be observed. Besides, methane concentration in the feed gas is usually as low as 1.0 vol.% due to the explosive limit of methane, in the range of 5–15 vol.% in air.

In general, catalysts for methane combustion can be divided into two groups, noble metals such as Pt, Pd, Rh, and Ru, and transition metal oxides such as  $\text{CO}_3\text{O}_4$ , CuO,  $\text{Cr}_2\text{O}_3$  and  $\text{MnO}_2$ . Several of the elements of the platinum group metals have an outstanding capability in oxidizing hydrocarbons as well as hydrogen and carbon monoxide. They have found widespread use as active materials in catalysts used at low to moderate temperatures [2], [3]. Among the noble metal-based catalysts, the activities of Pd and Pt are considered to be significantly higher than the others, and Pd-based catalysts always show the best activity in methane combustion. However, the supported noble metals catalysts, such as Pd and Pt, show a higher activity, but lower thermal stability, and the limited supply restricts the use of noble metals. In order to improve the thermal stability of the noble metal catalysts, researchers have paid much attention to studying the efficient support [4].

The most common catalyst for methane combustion at low temperatures is Pd loaded  $\gamma$ - $\text{Al}_2\text{O}_3$  catalyst due to its higher surface area, moderate chemical activity and lower cost. But transition alumina will transfer inevitably to corundum after calcination at higher temperature, while its surface area and pore volume decreases significantly. Therefore, more sustainable material with higher thermal stability has increase the interest of researchers.

In Malaysia, there are 3.2 million tonnes of palm kernels as

biomass residue generated yearly [5]. One of the applications of palm kernel biomass is to obtain biochar, a carbon rich product when thermal decomposition of palm kernel under limited supply of oxygen ( $O_2$ ) at a temperature lower than  $700^\circ C$  [6]. They are relatively inexpensive, possess a high surface area, allow easy recovery of supported metal by simple burn of the support, show chemical inertness both in acidic and basic media, and at the same time do not contain very strongly acidic centers on their surface, which could provoke undesirable side reactions during the catalytic run. These advantages have makes them attractive as support material [7].

The aim of this work is to compare the kinetic rate of reaction of CCM between two different supports,  $\gamma-Al_2O_3$  and biochar (Bc) for 2wt% Pd-based catalysts. Also, is to investigate the physical and chemical properties of catalysts over the catalytic reaction. The focus is on the heterogeneous reaction of the catalytic activity.

## II. EXPERIMENTAL

### A. Pretreatment of Raw Material

Palm kernel precursors were washed and dried and undergone carbonization process to produce biochar. About 50 g of the kernel materials were placed in the stainless-steel reactor. Purified nitrogen, as purge gas flowed through the reactor at a flow rate of  $150\text{ cm}^3/\text{min}$ . Carbonization process was carried out in a vertical tube furnace which allows increase the temperature from room temperature to  $700^\circ C$  with heating rate of  $10^\circ C/\text{min}$ . At  $700^\circ C$ , this temperature was held constant for 2 hour [8]. The reactor was leave to cool until room temperature, and resulting biochar was removed from the reactor. The biochar was grinded and sieved to the size of in between 28 mesh – 32 mesh which is approximate  $500\text{ }\mu\text{m}$ -  $600\text{ }\mu\text{m}$ . Fig. 1 shows the apparatus setup for carbonization process of palm kernel.

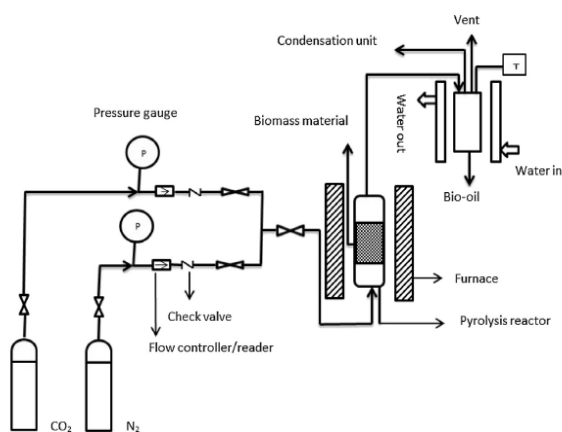


Fig. 1 Schematic diagram of Pyrolysis and Carbonization Processes for sustainable agro-base waste material

### B. wt% Pd/ $\gamma-Al_2O_3$

5g of palladium based catalyst support by alumina, 2 wt% Pd/ $\gamma-Al_2O_3$ , was prepared by incipient wetness impregnation

process with palladium nitrate dihydrate,  $Pd(NO_3)_2 \cdot 2H_2O$  precursor and  $\gamma$ -alumina. 0.25g of  $Pd(NO_3)_2 \cdot 2H_2O$  was dissolved in 5mL of ionized water and then impregnated onto the metal oxide supports. The mixture was stirred for 30 minute. The impregnated catalyst solution was filtered using filter paper and then dried for 6 hours at room temperature. After drying under room temperature, the impregnated catalyst was again dried using oven at  $100^\circ C$  for 24 hours [9].

### C. Calcined 2 wt% Pd/ $\gamma-Al_2O_3$

3 g of prepared 2 wt% Pd/ $\gamma-Al_2O_3$  in were used to undergo calcination process in air. At the beginning of the calcination process, impregnated catalyst was heated at a rate of  $4^\circ C/\text{min}$  until  $475^\circ C$ . The condition was kept constant for 4 hours and subsequently cooled at a rate of  $10^\circ C/\text{min}$  to  $25^\circ C$ .

### D. wt% Pd/Bc

4.9g of palladium based catalyst support by bio-char, 2 wt% Pd/ bio-char, was prepared using same method as previous catalyst preparation, incipient wetness impregnation process. Palladium nitrate dihydrate,  $Pd(NO_3)_2 \cdot 2H_2O$  precursor and bio-char. 0.25g of  $Pd(NO_3)_2 \cdot 2H_2O$  was dissolved in 5mL of ionized water and then impregnated onto the bio-char supports. The impregnated catalyst solution was filtered using filter paper and then dried for 6 hours at room temperature. After drying under room temperature, the impregnated catalyst was again dried using oven at  $100^\circ C$  for 24 hours.

### E. Calcined 2 wt% Pd/Bc

After the wet impregnation process, the calcination process in air was carried out. At the beginning of the calcination process, impregnated catalyst was heated at a rate of  $4^\circ C/\text{min}$  until  $475^\circ C$ . The condition was kept constant for 4 hours and subsequently cooled at a rate of  $10^\circ C/\text{min}$  to  $25^\circ C$ .

### F. Catalysts Characterization

Thermogravimetric analysis is done to analyze the thermal behavior of palm kernel. Thermogravimetric analysis (TGA) is also widely used to determine the thermal stability of the samples. It is based on the measurement of mass loss of material as a function of temperature. It was carried out by using Mettler Toledo TGA/DSC1 instrument with a heating rate of  $20^\circ C/\text{min}$  at a temperature range of  $25-400^\circ C$ , the thermograms were obtained. All TGA runs were performed under a nitrogen purge condition [10]. Scanning electron microscopy (SEM) was carried out before and after the catalytic reaction of methane. SEM instrument was used to analyse the morphological images and pore size of the solid sample materials. SEM Karl Zeiss (EVO50 XVPSEM, Germany) was used in this research for the scanning electron microscopy. Morphological views with different magnification of 500, 1,000 and 5000 were examined for each sample. Brunauer, Emmett and Teller (BET) method is used to measure the surface area of samples. These samples were prepared 2 wt% Pd/ $\gamma-Al_2O_3$ , prepared 2 wt% Pd/biochar and the reacted 2 wt% Pd/ $\gamma-Al_2O_3$ . The characterization of the three samples was performed after the catalysts preparation.

### G. Catalytic Reaction

Catalytic performances of calcined and prepared catalysts were tested through oxidation of methane. It was carried out in a tubular quartz reactor flowing through 100 ml/min of reacting mixture. Flow rate of CH<sub>4</sub> in feed stream was kept in the range of 3% ± 25 volume % concentration of mixture and the rest was air (76.63 ml/min N<sub>2</sub>; 20.37 ml/min O<sub>2</sub>) under stoichiometric conditions. Flow rate of CH<sub>4</sub> and air feed were controlled by digital mass flow controller. The ratio of reacting mixture as well as its flow rate was fixed constant throughout this study. A thermocouple was inserted into the reactor to measure the temperature of reaction. Before each experiment, catalyst was purged with N<sub>2</sub> (50 ml/min) for 15 min. After purging, the heater started to operate and reacting mixture was allowed to flow through at 100 °C for preheating.

The activities were evaluated between 0 – 100% of methane conversion. Online gas analyzer was connected to the inlet and outlet stream of reactor to detect the compositions of reacted flue gas respectively. Temperature ramped at the rate of 10°C/min for 10 minute and held for 15minute in each segment. During the holding time, result was recorded every 5 minute. The schematic diagram of methane combustion set-up is shown in Fig. 2. Reacted catalysts were collected and sent for characterization.

### H. Kinetic Evaluation of CCM

Reaction order for methane concentrations in the range 0.1-6 % volume is first order. Thus, the mass specific reaction rate constant (km) can be calculated as [1]:

$$Km = -\left(\frac{F}{m}\right) [\ln(1-x)] \quad (1)$$

where, F/m is volumetric feed rate of reactant divided by the weight of catalyst and x is methane conversion. The Arrhenius plot for each catalyst performance was developed below 50% methane conversion to achieve the kinetic regime, and to avoid the diffusion regime. The kinetic parameters of the activation energy, and pre-exponential factor were computed using (2);

$$k = Ae^{-\frac{E}{RT}} \quad (2)$$

where k is the specific reaction rate, cm<sup>3</sup>/g s, with temperature dependence, E is the activation energy, kJ/mol, A is the pre-exponential factor, or frequency factor, cm<sup>3</sup>/g s, R is a gas constant, 8.314 kJ/mol K, and T is absolute temperature, K. By taking natural logarithm as given in (3),

$$\ln k = \ln A - E/R\left(\frac{1}{T}\right) \quad (3)$$

An Arrhenius plot of k versus (1/T) should be a straight line whose slope is proportional to the activation energy, and A is computed at the y-axis when (1/T) is located to the origin point.

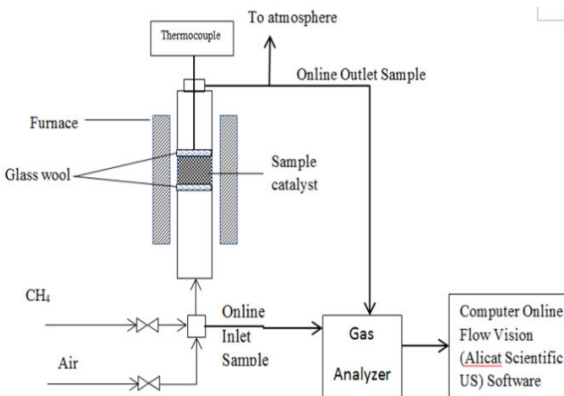


Fig. 2 Schematic diagram of catalytic reaction of methane

## III. RESULTS AND DISCUSSION

The TGA curves for palm kernel waste material obtained from the pyrolysis process are displayed in Fig. 3. From this experiment, the initial weight loss could be due to removal of water at 100°C, decomposition of cellulose at 280-300°C and decomposition of hemicellulose at 340–360°C. The reduced sample was stable at 30-600°C then started decomposing at 600-630°C [12]. Biochar was produced by carried out carbonization process of palm kernel at 700°C. The biochar formed at this temperature is thermally stable and without any volatile compound.

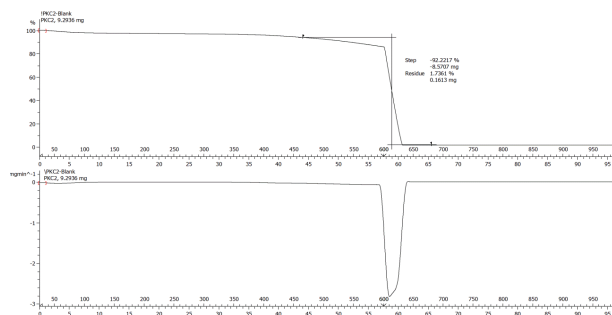


Fig. 3 TGA curve of palm kernel shell

Morphologies and distribution patterns of palladium in (a) prepared 2wt%Pd/γ- Al<sub>2</sub>O<sub>3</sub>, (b) reacted 2wt% Pd/γ- Al<sub>2</sub>O<sub>3</sub> and (c) prepared 2wt% Pd/Bc catalysts are shown in Figs. 4, 5. For catalysts (a) and (b) produced were in crystalline form. The crystalline shape enables the formation of crevices on the catalysts. In Fig. 4, channels can be seen between cracks on the catalyst surface. Sample (c) shown in Figs. 4, 5 was observed, the Pd metal catalyst was not well distributed on the surface of biochar support due to its complex porous structure and the pores between particles were not significantly shown.

BET surface area of the prepared 2wt% Pd/γ- Al<sub>2</sub>O<sub>3</sub> and reacted 2wt% Pd/γ- Al<sub>2</sub>O<sub>3</sub> (Table I) is relatively high compare to that of prepared 2wt% Pd/Bc. The large number of pores on each catalyst particle will provide larger surface area for the particle. The larger the surface area of the catalyst, the potential for reaction on the surface increases. This is so

because one of the factors influencing the reaction on the surface is the surface area of the catalyst.

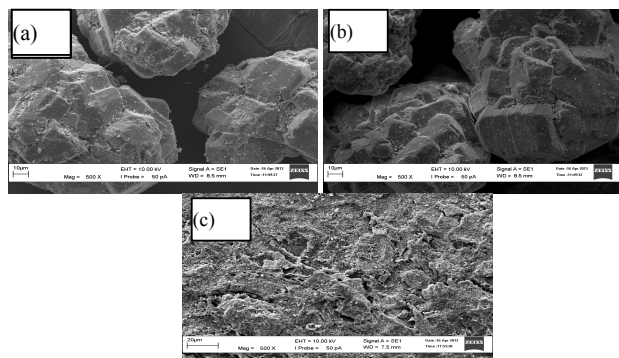


Fig. 4 Catalyst samples morphology effect (500 times) (a) prepared 2wt% Pd/  $\text{Al}_2\text{O}_3$ , (b) Reacted 2wt% Pd/ $\gamma$ -  $\text{Al}_2\text{O}_3$ , (c) prepared 2wt% Pd/Bc

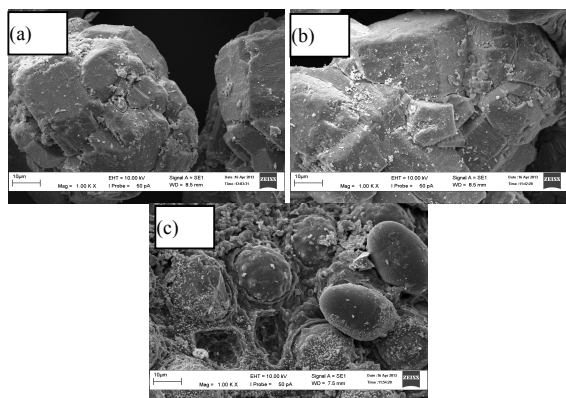


Fig. 5 Catalyst samples morphology effect (1000 times) (a) prepared 2wt% Pd/  $\text{Al}_2\text{O}_3$ , (b) Reacted 2wt% Pd/ $\gamma$ -  $\text{Al}_2\text{O}_3$ , (c) prepared 2wt% Pd/Bc

TABLE I

BET SURFACE AREA FOR PREPARED 2WT% Pd/  $\text{Al}_2\text{O}_3$ , REACTED 2WT% Pd/  $\text{Al}_2\text{O}_3$  AND PREPARED 2WT% Pd/Bc CATALYST

Sample	BET surface area ( $\text{m}^2/\text{g}$ )
Prepared 2wt% Pd/ $\text{Al}_2\text{O}_3$	124.74
Reacted 2wt% Pd/ $\text{Al}_2\text{O}_3$	110.99
Prepared 2wt% Pd/Bc	89.77

By comparing surface area of with prepared 2wt% Pd/ $\gamma$ - $\text{Al}_2\text{O}_3$  catalyst, reacted 2wt% Pd/ $\gamma$ -  $\text{Al}_2\text{O}_3$  catalyst was observed to have lower surface area. The reacted 2wt% Pd/ $\gamma$ - $\text{Al}_2\text{O}_3$  catalyst indicated a decreased in surface area after the reaction. Demoulin et al. reported after the CCM test at high temperature, sintering of palladium phase occur [13]. The tendency of particles to bind between each other after the catalytic reaction carried out has reduced the surface area of the reacted catalyst. The surface area of prepared 2wt% Pd/ $\gamma$ - $\text{Al}_2\text{O}_3$  catalyst was relatively large compare to that of prepared 2wt% Pd/Bc catalyst. It was expected to have small surface area due to its low porosity. The reason behind is biochar produced undergone carbonization process did not develop porous structure due to the blockage of the pores by tars. As a

result, the obtained dispersions tend to be relatively low and this contributed to a lower potential of reaction [14].

**Kinetic Analysis:** In order to evaluate catalytic activity on of catalysts under heterogeneous of CCM, T50 values (temperature at 50% of methane conversion) were calculated and reported in Table II.

TABLE II  
TEMPERATURE AT 50% OF METHANE CONVERSION

Catalysts	T <sub>50</sub> (K)
prepared 2wt% Pd/ $\gamma$ - $\text{Al}_2\text{O}_3$	603.3
calcined 2wt% Pd/ $\gamma$ - $\text{Al}_2\text{O}_3$	576.6
prepared 2wt% Pd/Bc	531.0
calcined 2wt% Pd/Bc	773.29

For kinetic model, the kinetic expressions to be used in the reactor have been shown in (2) and (3). A simple Arrhenius law was adopted for the variation of the constant. This equation was used to fit the experimental data (conversion versus temperature). From the integral conversion data the overall rate of reaction K, can be calculated. Function  $\ln(k)$  of (1/T) (in Kelvin) was then linearly regressed [12]. The linear graph in Fig. 6 is the exponential of Arrhenius plot for below 50% of methane conversion.

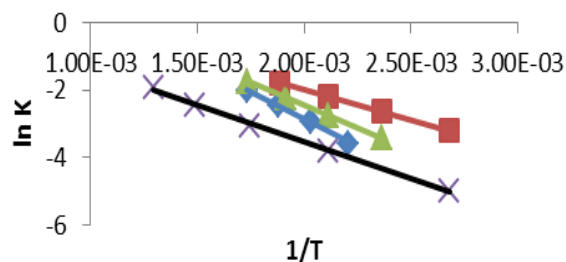


Fig. 6 Exponential Arrhenius plot of catalytic activity for (♦) prepared 2wt% Pd/ $\gamma$ -  $\text{Al}_2\text{O}_3$ , (▲) calcined 2wt% Pd/ $\gamma$ -  $\text{Al}_2\text{O}_3$ , (■) prepared 2wt% Pd/Bc and (x) calcined 2wt% Pd/Bc catalysts.

Among the four catalysts tested, prepared 2wt% Pd/ $\gamma$ - $\text{Al}_2\text{O}_3$  catalyst has the highest pre-exponential factor and activation energy (Table III). The higher the pre-exponential factor, the collision frequency between reactants molecules on surface of catalyst also increases. However, would require higher energy is in order to allow the heterogeneous reaction to occur due to its high activation energy. The activation energy was reported strongly depends on the reaction temperature and chemical state of palladium. The inhibition of oxygen uptake to form PdO would result an increase in activation energy for the oxidation reaction [15].

TABLE III  
SUMMARY OF PARAMETER PRE-EXPONENTIAL FACTOR, A AND ACTIVATION ENERGY, E OF CATALYSTS

Sample	A ( $\text{cm}^3/\text{g s}$ )	E (kJ/mol)
Prepared 2wt% Pd/ $\text{Al}_2\text{O}_3$	74.23	29.70
Prepared 2wt% Pd/Bc	4.62	14.69
Calcined 2wt% Pd/ $\text{Al}_2\text{O}_3$	17.66	22.14
Calcined 2wt% Pd/Bc	2.25	18.12

In contrast, prepared 2wt% Pd/Bc catalyst was observed to have the lowest pre-exponential factor and this can be concluded that the chances of collision between reactant and catalyst surface is very low. However the low activation energy enabled the initiation of heterogeneous reaction to occur at the lowest temperature and the methane conversion drastically increased compare to other samples (Fig. 7). This shows the activation energy of prepared 2wt% Pd/Bc is more dominant. It is suggests that metal catalyst Pd lower the activation energy not only for CH<sub>4</sub> and O<sub>2</sub> reactants but also the activation energy between carbon and oxygen element in the biochar support.

In comparison with prepared 2wt% Pd/ $\gamma$ -Al<sub>2</sub>O<sub>3</sub>, the calcined 2wt% Pd/ $\gamma$ -Al<sub>2</sub>O<sub>3</sub> would have better performance. The pre-exponential factor is much lower than prepared 2wt% Pd/ $\gamma$ -Al<sub>2</sub>O<sub>3</sub> probably due to the reduction of surface area caused by sintering effect during calcination. However, with relatively low activation energy as the dominant factor, the calcined 2wt% Pd/ $\gamma$ -Al<sub>2</sub>O<sub>3</sub> has increased methane conversion at low temperature.

TABLE IV  
KINETIC RATE OF REACTION AT THREE DIFFERENT TEMPERATURES

Temperature (K)	Kinetic rate of reaction, K (cm <sup>3</sup> /g s)			
	prepared 2wt% Pd/ $\gamma$ -Al <sub>2</sub> O <sub>3</sub>	calcined 2wt% Pd/ $\gamma$ -Al <sub>2</sub> O <sub>3</sub>	prepared 2wt% Pd/Bc	calcined 2wt% Pd/Bc
373	0.01	0.01	0.04	0.01
473	0.04	0.06	0.11	0.02
573	0.15	0.17	0.21	0.05

The kinetic rate of reaction, K of each catalyst at three different temperatures below T50 was calculated and tabulated in Table IV. The results clearly indicate the performance of catalysts under heterogeneous reaction at temperature below T50. That is, the catalyst with higher kinetic rate of reaction would have higher catalytic activity. Obviously, the order of kinetic rate of reaction of catalyst at any temperature under the same condition, T50, (Fig. 8) is prepared 2wt% Pd/Bc > calcined 2wt% Pd/ $\gamma$ -Al<sub>2</sub>O<sub>3</sub> > prepared 2wt% Pd/ $\gamma$ -Al<sub>2</sub>O<sub>3</sub> > calcined 2wt% Pd/Bc.

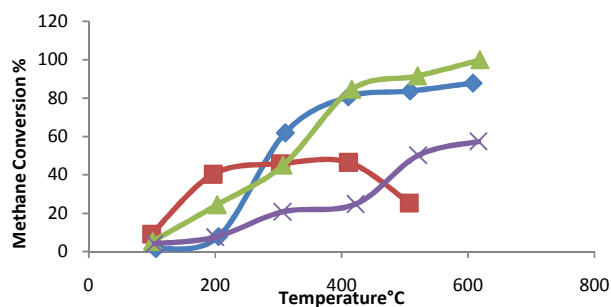


Fig. 7 Methane conversion as a function of temperature for (♦) 2wt% Pd/ $\gamma$ -Al<sub>2</sub>O<sub>3</sub>, (▲) calcined 2wt% Pd/ $\gamma$ -Al<sub>2</sub>O<sub>3</sub>, (■) 2wt% Pd/Bc and (x) calcined 2wt% Pd/Bc catalysts

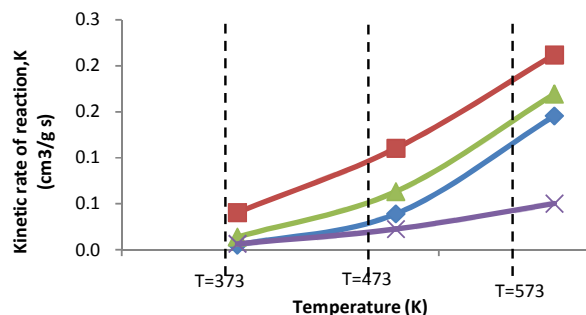


Fig. 8 Kinetic rate of reaction of (♦) prepared 2wt% Pd/ $\gamma$ -Al<sub>2</sub>O<sub>3</sub>, (▲) calcined 2wt% Pd/ $\gamma$ -Al<sub>2</sub>O<sub>3</sub>, (■) prepared 2wt% Pd/Bc and (x) calcined 2wt% Pd/Bc catalysts at temperature, T =373K, 473K, 573K

Flue Gas Analysis: The flue gases, in volume basis were detected from the catalytic reaction by using online gas analyzer. The composition of CH<sub>4</sub>, O<sub>2</sub>, CO, CO<sub>2</sub> gases released against temperature by catalytic reaction on each catalyst that has been tested is plotted in Figs. 9–12. Each respective catalyst will be analyzed based on low temperature regime that is at methane conversion below 50%.

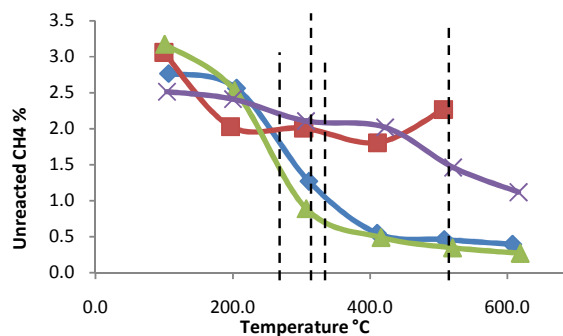


Fig. 9 Composition of CH<sub>4</sub> as a function of temperature for (♦) prepared 2wt% Pd/ $\gamma$ -Al<sub>2</sub>O<sub>3</sub>, (▲) calcined 2wt% Pd/ $\gamma$ -Al<sub>2</sub>O<sub>3</sub>, (■) prepared 2wt% Pd/Bc and (x) calcined 2wt% Pd/Bc catalysts

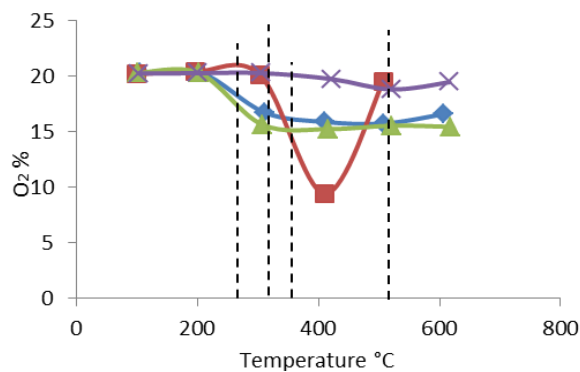


Fig. 10 Composition of O<sub>2</sub> as a function of temperature for (♦) prepared 2wt% Pd/ $\gamma$ -Al<sub>2</sub>O<sub>3</sub>, (▲) calcined 2wt% Pd/ $\gamma$ -Al<sub>2</sub>O<sub>3</sub>, (■) prepared 2wt% Pd/Bc and (x) calcined 2wt% Pd/Bc catalysts

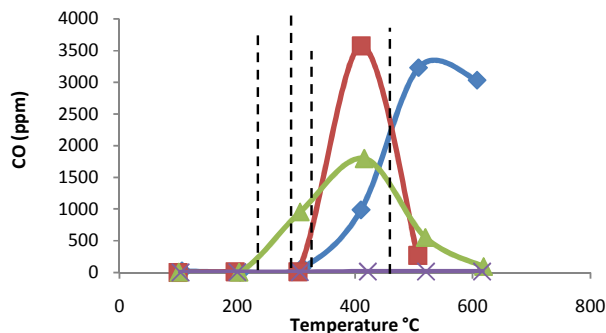


Fig. 11 Composition of CO as a function of temperature for (♦) prepared 2wt% Pd/  $\gamma$ -  $\text{Al}_2\text{O}_3$ , (▲) calcined 2wt% Pd/  $\gamma$ -  $\text{Al}_2\text{O}_3$ , (■) prepared 2wt% Pd/Bc and (x) calcined 2wt% Pd/Bc catalysts

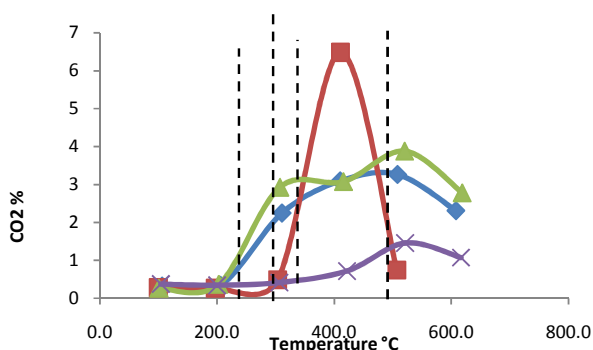


Fig. 12 Composition of  $\text{CO}_2$  as a function of temperature for (♦) prepared 2wt% Pd/  $\gamma$ -  $\text{Al}_2\text{O}_3$ , (▲) calcined 2wt% Pd/  $\gamma$ -  $\text{Al}_2\text{O}_3$ , (■) prepared 2wt% Pd/Bc and (x) calcined 2wt% Pd/Bc catalysts

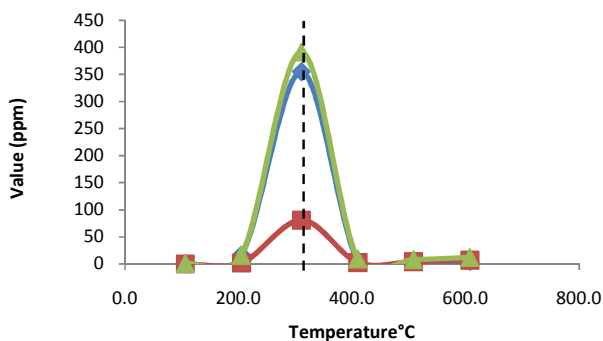


Fig. 13 Composition of (♦) NO, (■)  $\text{NO}_2$  and (▲)  $\text{NO}_x$  emission as a function of temperature for prepared 2wt% Pd/  $\gamma$ -  $\text{Al}_2\text{O}_3$

Prepared 2wt% Pd/  $\gamma$ -  $\text{Al}_2\text{O}_3$ : At low temperature around 200°C, composition of  $\text{CH}_4$  in flue gases decreased and small amount of  $\text{CO}_2$  were observed. There was no CO detected in flue gases. In addition, the composition three gases NO,  $\text{NO}_2$  and  $\text{NO}_x$  were extremely low as shown in Fig. 13. Therefore the reaction is said to be a complete reaction. Then, reaction was continued until T50 at around 330°C. Slightly below the T50, the emissions of CO and  $\text{CO}_2$  have started to increase. The three gases NO,  $\text{NO}_2$  and  $\text{NO}_x$  exhibited the similar behavior where the peak of each graph was at the temperature

around 310°C. However  $\text{NO}_x$  and NO gaseous released at that point were relatively high compare to that of  $\text{NO}_2$  gas. The overall reaction has entered the transition from kinetically control to mass transfer control at before T50. The mass transfer control could be due to intraparticle pore diffusion limitation, as well as the interparticle transfer of methane to the catalyst surface [15].

Calcined 2wt% Pd/  $\gamma$ -  $\text{Al}_2\text{O}_3$ : For calcined 2wt% Pd/  $\gamma$ -  $\text{Al}_2\text{O}_3$  catalyst, the composition of both CO and  $\text{CO}_2$  emissions from reaction were similar to prepared 2wt% Pd/  $\gamma$ -  $\text{Al}_2\text{O}_3$  catalyst at 200°C. However, as temperature increased, the  $\text{CH}_4$  and  $\text{O}_2$  released were decreasing faster than that of the prepared 2wt% Pd/  $\gamma$ -  $\text{Al}_2\text{O}_3$  catalyst. The incomplete reaction led to CO and  $\text{CO}_2$  emissions increased with temperature and they showed a higher rate compared to the prepared 2wt% Pd/  $\gamma$ -  $\text{Al}_2\text{O}_3$  catalyst. Besides that, the peak of NO and  $\text{NO}_x$  emission occurred at around its T50 as shown in Fig. 14. Whereas the  $\text{NO}_2$  emissions increased as temperature increased. However the overall NO,  $\text{NO}_2$  and  $\text{NO}_x$  is relatively low compare to the prepared 2wt% Pd/  $\gamma$ -  $\text{Al}_2\text{O}_3$ . This is because the calcined 2wt% Pd/  $\gamma$ -  $\text{Al}_2\text{O}_3$  catalyst has a higher catalytic activity than the prepared 2wt% Pd/  $\gamma$ -  $\text{Al}_2\text{O}_3$  at low temperature. Therefore, the reaction reached to the transition stage between two kinetic and mass transfer controls earlier.

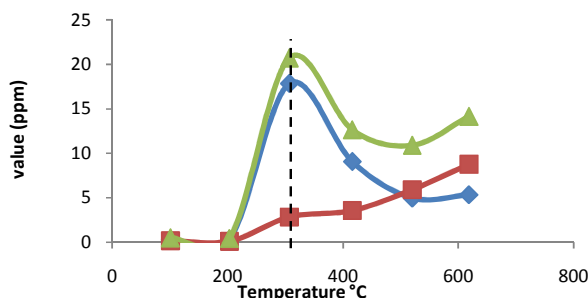


Fig. 14 Composition of (♦) NO, (■)  $\text{NO}_2$  and (▲)  $\text{NO}_x$  as a function of temperature for Calcined 2wt% Pd/  $\gamma$ -  $\text{Al}_2\text{O}_3$  catalyst

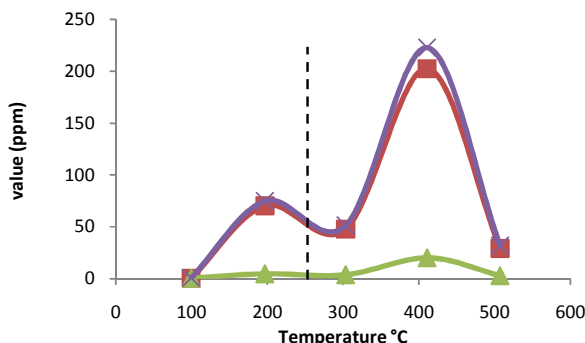


Fig. 15 Composition of (■) NO (▲)  $\text{NO}_2$  and (x)  $\text{NO}_x$  emission as a function of temperature for prepared 2wt% Pd/Bc catalyst

Prepared 2wt% Pd/Bc: Prepared 2wt% Pd/Bc catalyst has showed an excellent performance at low temperature. At the

initiation of reaction, the composition of released CH<sub>4</sub> in flue gases was drastically decreased. Small amount of CO<sub>2</sub> was formed and there was no CO emission detected during the reaction. The NO, NO<sub>2</sub>, NO<sub>x</sub> emissions (Fig. 15) were low compared to the prepared 2wt% Pd/ $\gamma$ -Al<sub>2</sub>O<sub>3</sub> catalyst. As a result, under the same condition that is T50, prepared 2wt% Pd/Bc showed the highest catalytic activity. So biochar (Bc) is more excellent than  $\gamma$ -Al<sub>2</sub>O<sub>3</sub> for Pd based catalyst at low temperature regime in methane combustion.

Calcined 2wt% Pd/Bc: For calcined 2wt% Pd/Bc, the CH<sub>4</sub> and O<sub>2</sub> in flue gas were high over a big range of reacting temperature. In other words, at low temperature, only small amount of CH<sub>4</sub> and O<sub>2</sub> were consumed during the reaction. However, at below T50, no CO was produced throughout the reaction and most importantly the emission of NO, NO<sub>2</sub> and NO<sub>x</sub> gases as shown in Fig. 16 were significantly low.

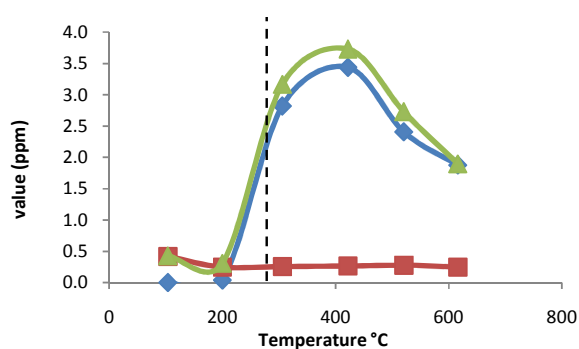


Fig. 16 Composition of (♦) NO, (■) NO<sub>2</sub> and (▲) NO<sub>x</sub> as a function of temperature for Calcined 2wt% Pd/Bc

#### IV. CONCLUSION

In this study, 2 wt% Pd/ $\gamma$ -Al<sub>2</sub>O<sub>3</sub>, reacted 2 wt% Pd/ $\gamma$ -Al<sub>2</sub>O<sub>3</sub> and 2wt% Pd/Bc were characterized using SEM and BET surface area to study the morphology and surface area of the catalyst respectively. The morphology of catalysts shows that porosity of particles had much influence on their surface area. The order of BET surface area for characterized catalysts are prepared 2 wt% Pd/ $\gamma$ -Al<sub>2</sub>O<sub>3</sub> > reacted 2 wt% Pd/ $\gamma$ -Al<sub>2</sub>O<sub>3</sub> > prepared 2wt% Pd/Bc. Furthermore, the performance of prepared 2 wt% Pd/ $\gamma$ -Al<sub>2</sub>O<sub>3</sub>, calcined 2 wt% Pd/ $\gamma$ -Al<sub>2</sub>O<sub>3</sub>, prepared 2 wt% Pd/Bc and calcined 2 wt% Pd/Bc catalysts under heterogeneous reaction of CCM was studied. The results show that, at low temperature regime, prepared 2 wt% Pd/Bc has the highest catalytic activity among the others, followed by calcined 2 wt% Pd/ $\gamma$ -Al<sub>2</sub>O<sub>3</sub>, prepared 2 wt% Pd/ $\gamma$ -Al<sub>2</sub>O<sub>3</sub> then calcined 2 wt% Pd/Bc. Despite the low pre-exponential factor of prepared 2 wt% Pd/Bc, its low activation energy has become dominant factor over the heterogeneous reaction. However, more research is to be carried out to determine the life of support material and its thermal stability at high temperature.

#### ACKNOWLEDGMENT

The authors appreciate and thank the financial support and contribution provided by the Ministry of Education (MOE), Malaysia and Universiti Teknologi Malaysia through the Research University Grant (GUPT1) Q.J130000.2509.06H79. Special an appreciation to the Sustainability Waste-To-Wealth Unit of UTM-MPRC Institute for Oil and Gas, Universiti Teknologi Malaysia to provide technical supports.

#### REFERENCES

- [1] IPCC, "Summary for Policymakers. In: Climate Change 2007: The Physical Science Basis". Cambridge: Cambridge University Press. 2007.
- [2] T. Philippe T. Catalytic Combustion of Methane. Doctor Philosophy, Kungliga Tekniska Högskolan, Stockholm. 2002.
- [3] G. Guoqing, K. Kusakabe, M. Taneda, M. Uehara and H. Maeda. J. Chem. Eng. 144: 270-276. 2008.
- [4] X. H. Wang, G. Z. Guo, Y. Lu, L. Z. Hu, Y.L. Jiang, Z. Guo, and G. Zhang. Catal. Today, 126:369-374. 2007.
- [5] A. M. Fadzil and U. A. M. Hakimi. Utilization of biomass residues for optimization of municipal solid waste combustion, Proceedings of the Advances in Malaysian Energy Research, pp. 9-16. 2004.
- [6] J. Lehmann, S. Joseph. Biochar for environmental management. Washinto, Earthscan. 2009.
- [7] M. Gurratha, T. Kuretzka, H. P. Boehm, L. B. Okhlopkova, A.S. Lisitsyn, V. A. Likhobobov. Carbon. 38:1241-1255. 2000.
- [8] E. Koichi and A. Hiromichi. Appl. Catal. A. 222, 359-367. 2001.
- [9] O. Demoulin, G. Rupprechter, I. Seunier, B. Le Clef, M. Navez, and P. Ruiz. J. Phys. Chem. B. 109, 20454-20462. 2005.
- [10] N.S. Nasri and A. Abdul Kadir. Carbon Dioxide Adsorption and Desorption on Pre-treated Hydrophilic Property on Sustainable Pyrolysis Material of Bio-solid Waste, Universiti Teknologi Malaysia. 2012.
- [11] N. S. Nasri, J. M. Jones, V. A. Dupont, and A. Williams. A Comparative Study of Sulfur Poisoning and Regeneration of Precious-Metal Catalysts. Energy & Fuels. 12(6), 1130-1134. 1998.
- [12] Z. Khan, S. Yusupand M. M. Ahmad. Thermogravimetric Analysis of Palm Oil Wastes Decomposition. 2011 Ieee First Conference On Clean Energy And Technology Cet. 27-29 June. Kuala Lumpur, Malaysia: IEEE, 205-208. 2011.
- [13] O. Demoulin, G. Rupprechter, I. Seunier, B. Le Clef, M. Navez and P. Ruiz. Investigation of Parameters Influencing the Activation of a Pd/T-Alumina Catalyst during Methane Combustion. J. Phys. Chem. 109, 20454-20462. 2005.
- [14] F. Rodriguez-Reinoso and M. M. Sabio. Textural and Chemical Characterization of Microporous Carbons. Advances in Colloid and Interface Science. 76-77, 271-294. 1998.
- [15] Y. Chin and D.E. Resasco. Catalytic Oxidation of Methane on Supported Palladium under Lean Conditions: Kinetics, Structure and Properties. Catalysis. 14, 1-39. 1999.